Thermal Runaway Characteristics of Silicon Microstrip Module Designed for ATLAS Upgrade Inner Tracker at Super LHC

T. Kohriki, S. Terada, Y. Unno, Y. Ikegami, and K. Hara

***Abstract*- In accordance with the super LHC program, which plans to increase a collision rate of LHC by tenfold, the ATLAS silicon strip trackers need to be upgraded to overcome proportionally higher data rate and harsher radiation environment. Immediate concern is an increase of leakage current induced by radiation damage under such a severe condition. Without proper thermal management increase of the leakage current might lead silicon tracker modules to a catastrophic thermal runaway. Considering that the ATLAS inner trackers are strictly required to be as thin as possible in radiation length, careful optimization is imperative to cope with a robust thermal performance against thermal runaway.**

Based on the present ATLAS silicon strip modules (SCT), we have designed an upgrade silicon module, which consists of large area silicon sensors with short readout strips and densely populated readout ASIC's. Thermal performance of such a module is investigated employing three dimensional FEA thermal analyses as well as a prototype thermal module. Although the upgrade module is about five times denser in readout channels than the present SCT, it shows a good thermal performance even with module materials comparable to the present SCT.

I. INTRODUCTION

RESPONDING to the super LHC program, which plans to extend a collision rate of LHC by tenfold [1], the ATLAS silicon microstrip trackers (SCT) need to be upgraded so as to handle proportionally higher data rate and harsher radiation environment. Particularly concerned is an increase of leakage current induced by radiation damage due to high intensity beam operation. Without proper thermal management the increase of the leakage current might lead silicon tracker modules to a catastrophic thermal runaway.

Since it is mandatory for the ATLAS inner trackers [2] that their materials should be minimized as much as possible in radiation length, careful optimization is imperative in designing the tracker modules to cope with a robust thermal performance against thermal runaway.

In order to verify robustness of thermal behavior of the module, we have fabricated a realistic thermal module. Detailed FEM thermal analyses using ANSYS program [3] was also conducted to reproduce the thermal module measurements.

Manuscript received November 14, 2008.

T. Kohriki, Y. Ikegami, Y. Unno and S. Terada (e-mail: susumu.terada@kek.jp) are with Inst. of Particle and Nuclear Studies, High Energy Accelerator Research Org., KEK, Tsukuba, Ibaraki 305-0801 Japan.

K. Hara is with Institute of Pure and Applied Sciences, University of Tsukuba, Tsukuba, Ibaraki 305-8571 Japan.

II. RADIATION DAMAGE AND THERMAL RUNAWAY

One of the most critical issues is how to overcome ten times harsher radiation environment. Immediate concern in operating a silicon detector is an increase of the leakage current, which is proportional to an accumulation of radiation dose [4]. The leakage current can be estimated by taking a damage constant of 4×10^{-17}A/cm. The expected dose accumulation in about five years of operation of the super LHC is 1 x 10^{15} 1MeV n-eq./cm^2 including a safety factor of two at 30cm from the collision point [5].

With this condition, the heat generation in a 0.3mm thick silicon sensor reaches about 1mW/mm^2 in reduction to the reference temperature of 0℃. As the leakage current increases, the silicon sensors heat up with an ohmic heat generation. An exponential rise of the leakage current as an increase of temperature invokes a catastrophic thermal behavior called thermal runaway, in which the module is heating up abruptly once it goes beyond some critical temperature.

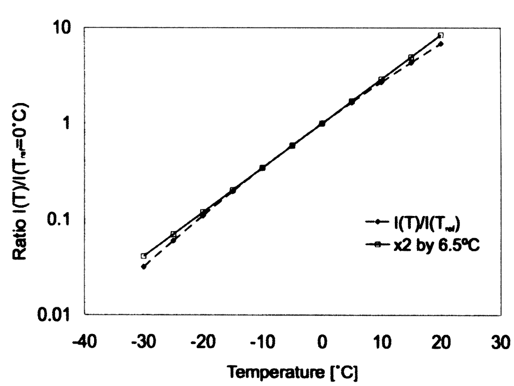

Fig. 1. Temperature dependence of leakage current of silicon sensors

The temperature dependence of the leakage current in silicon is formulated as in the following [6],

$$I(T) = I(T_{ref}) \cdot (T/T_{ref})^2 \exp\{-E_g/2k_B \cdot (1/T - 1/T_{ref})\}, \quad (1)$$

where T_{ref} is an arbitrarily chosen reference temperature. E_g and k_B are the silicon band gap and Boltzmann constant, respectively. This formula can be approximated to a simple exponential function,

$$I(T) \approx I(T_{ref}) \cdot 2^{(T-T_{ref})/T_{half}}. \quad (2)$$

They are plotted in Fig. 1. From this plot, we observe the leakage current changes by a factor of two as the temperature changes by 6.5˚C in the region around 0˚C. Therefore, the silicon detectors for the super LHC need to be farther cooled by about 20˚C to keep the heat generation in the silicon sensors at the same level of those for the LHC. Thus, the cooling temperature for the upgrade SCT module may become about -30˚C rather than -10˚C for the present SCT.

III. ATLAS SCT Upgrade Barrel Module

Based on the experience to develop the present ATLAS SCT [7], we have designed a silicon microstrip module for the upgraded ATLAS inner tracker for the super LHC. The silicon sensors can be fabricated from 6-inch wafers. From single 6-inch wafer, one square sensor of 9.8 cm x 9.8 cm is laid out. Four sections of 2.4 cm strip elements are embedded in the single sensor. Two sensors are glued back-to-back on a thermo-mechanical baseboard, similar to the present SCT barrel module.

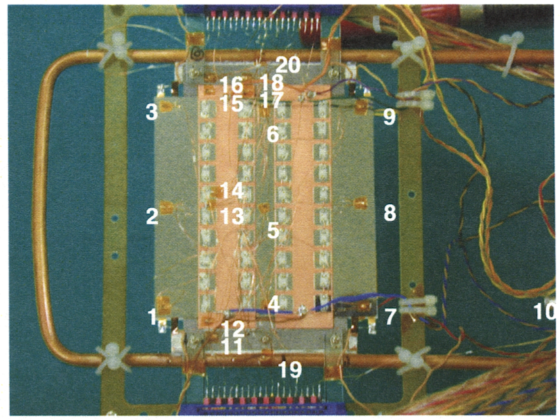

Fig. 3. Setup for the thermal module measurements; numbers denote thermocouples

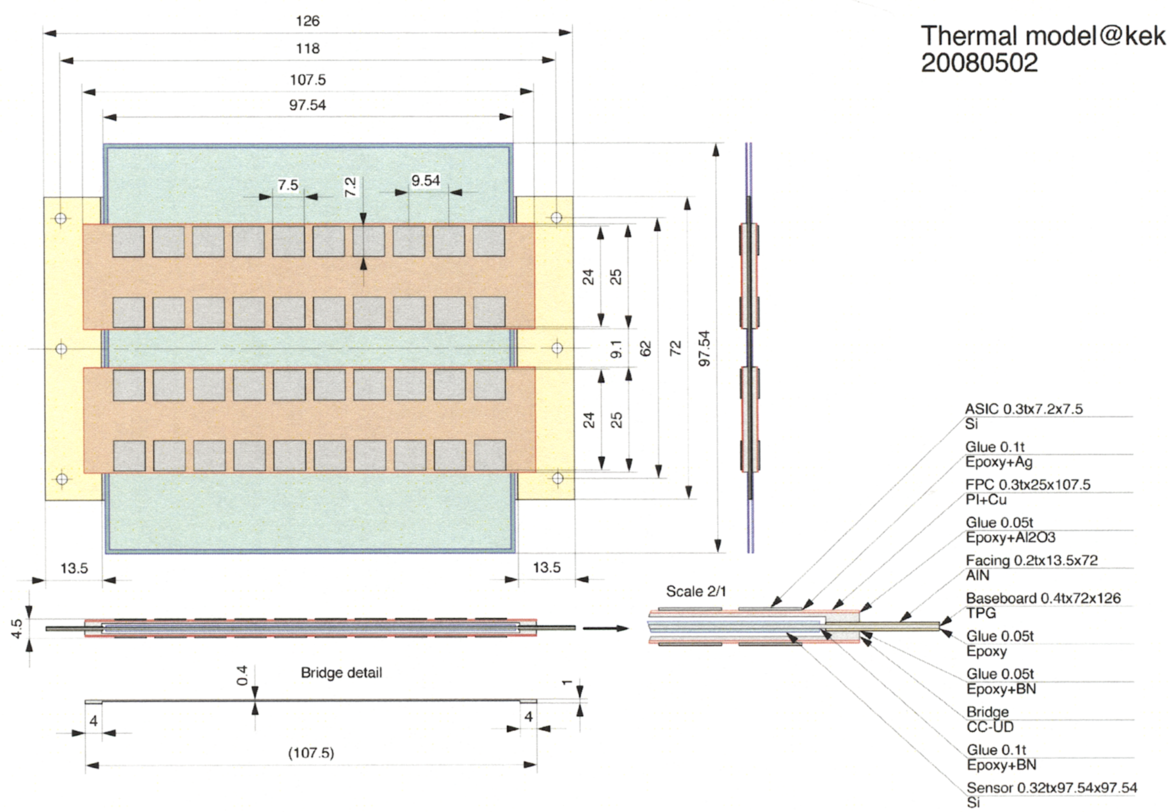

Fig. 2. Drawing of the thermal module for the ATLAS upgrade SCT barrel module

Since we have four sections of short strips in each sensor, the readout ASIC's of four rows have to be populated on hybrids. One hybrid serves for two rows, so we need two hybrids on each side (four hybrids per module). The hybrids are bridged over the sensors and attached to the extension of the baseboard at both ends, where the module is interfaced to cooling services. The drawing of the module is shown in Fig. 2.

IV. Thermal Module Measurements

Following the drawing (Fig. 2), a thermal module was fabricated as realistic as possible to investigate thermal performance. The thermal module consists of high resistive silicon plates and resistor chips instead of real sensors and ASIC's, respectively. Other critical components, however, such as the TPG base board, AlN ceramic facings and copper polyimide hybrids backed with CC bridges are exactly the same material to be used for the real module. The top and bottom surfaces of the silicon plates are aluminum metalized so as to apply voltage uniformly between them to generate ohmic heat.

The thermal module was set in a vacuum tight vessel and cooled with anti-freeze coolant. As shown in Fig. 3, a set of pt-100 thermocouples was attached on the module to measure temperature at various places. The numbers on the figure designate the places for those thermocouples.

The measurements were carried out in vacuum condition as well as nitrogen atmosphere. Results are shown in Fig.'s 4 (vacuum) and 5 (nitrogen).

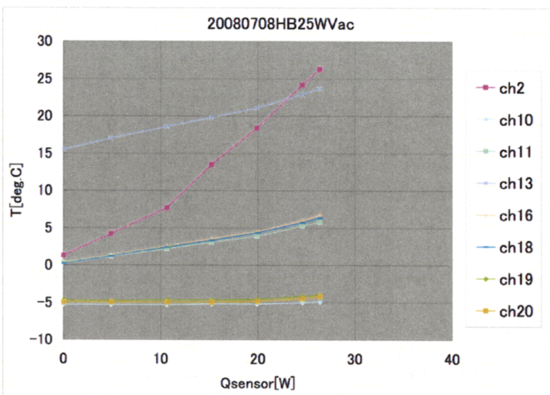

Fig. 4. Thermal module measurements in vacuum: silicon edge (CH2), middle ASIC (ch13), facing (CH11, 16, 18), ambient (CH10); Those channel numbers are corresponding to the thermocouples in Fig. 3.

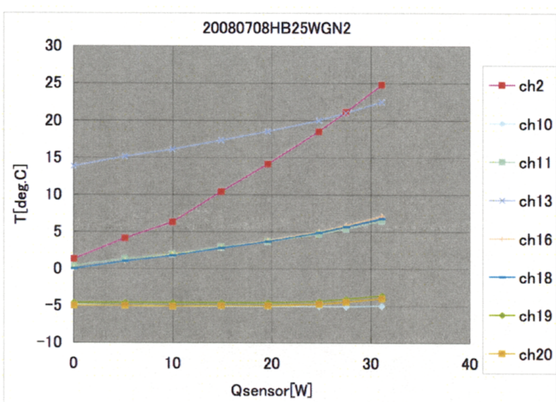

Fig. 5. Thermal module measurement in 1 atm nitrogen atmosphere; Channel numbers are explained in the caption for Fig. 4.

Plotted in the figures are temperatures of some representative points, namely silicon sensor edge (CH2), middle ASIC (CH13), cooling pipe (CH19, 20), facing (CH11, 16, 18) and ambient (CH10).

In the vacuum the runaway occurred at silicon power of 27W while it was 31W in the 1 atm nitrogen atmosphere. This discrepancy is due to convection heat transfer, which was confirmed by using Peltier cooler units. Required cooling power of the Peltier units to prevent the module temperature changing from vacuum to nitrogen was about 4W. This was also checked by ANSYS calculations with convection load.

Radiation heat transfer was estimated using a simple analytic model. Since the silicon plates are metalized and the whole module is enclosed in the stainless steel vacuum vessel, of which inner surface is polished and cleaned, the radiation effect is calculated to be negligibly small of about 0.1W.

V. FEM Thermal Analyses

Following the drawing (Fig. 2) in detail a three-dimensional model is constructed for ANSYS calculations to compare the results of the measurements as well as to estimate a runaway point. Cooling condition is set at -6.7℃ at the outer surface of the cooling pipe to reproduce the measurements. It is also set at -30℃ to obtain a runaway point in the operating condition for the super LHC.

Fig. 6 shows an isothermal contour of the module just before the runaway. Temperatures of some representative

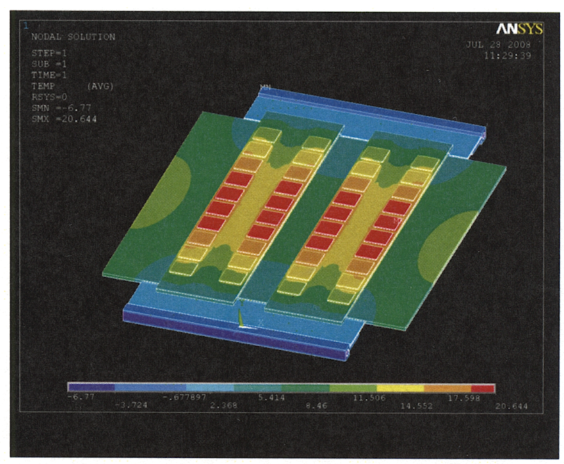

Fig. 6. Isothermal contour of the module just before runaway

points are plotted in Fig. 7 as a function of total sensor power to compare with the measurements. Three curves denoted as silicon, ASIC and facing are corresponding to CH2,CH13 and CH16 , respectively, in the measurements (Fig.'s 4 and 5). Runaway behaviors are plotted in Fig. 8 as a function of unit area silicon power in reduction to 0℃. The ANSYS results show a runaway point at 17W, which is somewhat with less power than the thermal module measurements. This may be explained by that, considering the large electric current of around 4A applied in the measurements, wirings and contact resistance of connections to the silicon plates might need extra power to dissipate, and also many thermocouples transfer some amount of heat power.

The effect of convection is analyzed by turning on a surface convection as an additional heat load in ANSYS calculation. Silicon surfaces and all ASIC top surfaces are subjected to the convection. As used for a film coefficient of $15W/m^2/K$ on those surfaces, additional required power needed for the runaway is about 4W, which is consistent with the Peltier measurements.

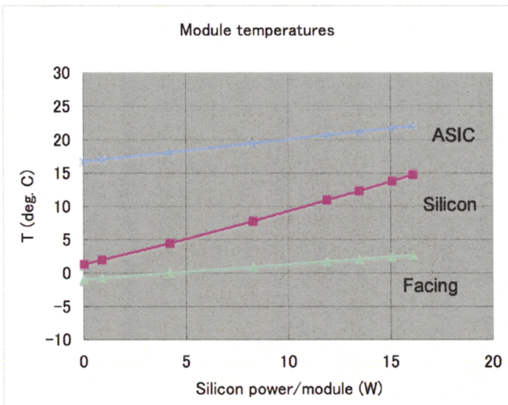

Fig. 7. Temperatures of representative points as a function of total silicon power; Three curves denoted as ASIC, Silicon and Facings are corresponding to CH13, CH2 and CH16 in Fig.'s 4 and 5, respectively.

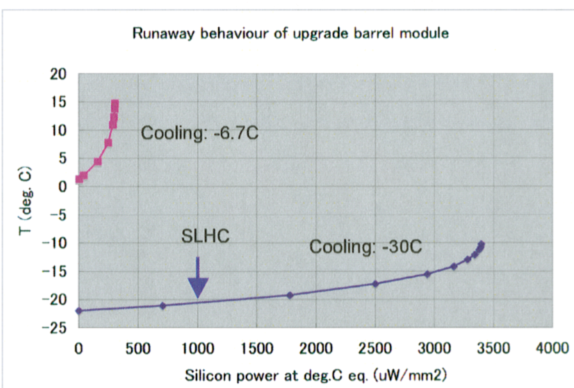

Fig. 8. Runaway behavior of the module with cooling temperatures of -6.7℃ and -30℃

The results with -30℃ cooling show that the runaway point is about $3{,}400\mu W/mm^2$ at 0℃ equivalent, which is more than three times larger than the requirement to the sensor heat power tolerance of $1{,}000\ \mu W/mm^2$ at 0℃ equivalent.

VI. Conclusions

We have proposed a silicon detector module for the upgraded ATLAS central tracker for the super-LHC. The module is designed to be structurally a natural extension of the present ATLAS SCT barrel module.

In order to investigate thermal performance, the thermal module measurements as well as the elaborated three-dimensional FEM analyses were carried out. The measurements together with the FEM analyses showed a good thermal behavior of the module. The runaway point obtained with the FEM analysis with -30℃ cooling is sufficiently larger than the required runaway criteria for the upgrade SCT barrel module with a comfortable safety margin of 3.4. Therefore it can be concluded that, by carefully choosing materials, for instance highly thermal conductive TPG baseboard and bridged hybrids with CC plate backings, although the upgrade module is about seven times denser in readout channels than the present SCT, it can be achievable a good thermal performance even with a total module material as thin in radiation length as that of the present SCT.

VII. References

[1] O. Bruning et al., LHC luminosity and energy upgrade: a feasibility study, LHC project report 626, CERN 2002; other latest references can be reached in the URL: http://care-hhh.web.cern.ch/care-hhh/publications.htm

[2] ATLAS Inner Detector Technical Design Report, Vol. I, ATLAS TDR4, CERN/LHCC 97-16, and Vol. II, ATLAS TDR5, CERN/LHCC 97-17.

[3] ANSYS Multiphysics, ANSYS, Inc.

[4] M. Moll, PhD thesis (1999), University of Hamburg, p99

[5] S. Baranov et al., ATL-GEN-2005-001, CERN, and the URL: http://dawson.web.cern.ch/dawson/fluka/index.html

[6] S.M. Sze, Physics of Semiconductor Devices, 2nd ed., John-Willy & Sons, p91 and associated equations

[7] T.Kondo et al., Nucl. Instr. Meth. A485 (2002) 27-42; A. Abdesselam et al, Nucl. Instr. Meth. A568 (2006) 642-671J.